of the main geometric and geomaterial parameters, but without considering the potential time-dependent deformations (creep effect) that occur in some types of rock masses.

Chen et al. [9], through analytical solutions in elasticity using complex variables, Fourier transformation, and the alternating Schwarz method, demonstrate that the mutual interaction between twin tunnels disappears if the spacing between the tunnels is greater than six times the tunnel radius. The lining effectively reduces the stress concentration, especially at high lateral stress coefficients.

Guo et al. [17] develop an elastic analytical solution for the stress field around twin circular tunnels with hydrostatic pressure using the complex variable and the superposition principle. They found that stress concentration in tunnel wall increased as the distance between the parallel tunnels decreased and the supporting pressure leads to the radial stress increasing and the tangential stress decreasing.

Ma et al. [18] proposed an analytical method, verified by a numerical solution using FLAC3D software for determining the plastic zones around deep circular twin tunnels without linings, restricting themselves where there is no overlap between the two plastic zones. In this case, the authors adopted the elastoplastic perfectly constitutive model for the homogeneous and isotropic rock mass, with the Mohr-Coulomb criterion. Also carried out parametric studies to understand the influence of the distance between the twin tunnels, cohesion, the angle of internal friction, and the vertical and horizontal initial stresses acting on the shape and depth of the plastic zones. These authors stated that the plastic zone around the tunnel provides a relevant theoretical basis for defining and designing the support. In that respect, an excessive plastic zone would significantly affect the stability and functionality of a tunnel. Reducing the extension of the plastic zone around tunnels is, therefore, of great importance in engineering tunnel design projects.

Using parametric three-dimensional numerical analyses, Chortis and Kavvadas [12, 13] investigated the effect of building a transverse tunnel that intersected deep twin tunnels perpendicularly, focusing the study on the axial forces and the circumferential and longitudinal bending moments acting on the primary support of the intersection regions, respectively. According to the authors, the potential interaction between deep twin tunnels lined with shotcrete must be taken into account, especially when the distance between them is less than or equal to twice their diameter.

According to Fortsakis [15], in a realistic construction context, twin tunnels are excavated and supported with a delay, so that the second tunnel is usually built after the first one has advanced enough to maintain a longitudinal separation distance between the faces. The advance of the subsequent tunnel mobilizes the redistribution of stresses and deformations in the zone between the tunnels, resulting in additional loading of the preceding tunnel.

As for transverse tunnels, these are generally built far enough behind the advanced face of the main tunnel to ensure that their excavation has virtually no effect during the construction of the junction tunnel [10]. The interaction at the intersection, between the main tunnel and the transverse tunnel, significantly modifies the stress state of the primary support and that of the surrounding rock mass in these areas, compared to that of the singular tunnel, making three-dimensional finite element analyses essential for developing a realistic and safe design for tunnel junctions [29].

During the construction of the transverse tunnel, the surrounding rock mass is subjected to a redistribution of stresses, causing an additional load on the main tunnel, precisely in the intersection zone. If these additional loads exceed the load capacity of the primary support of the main tunnel, a potentially unstable region can develop, leading to failure, especially in adverse geotechnical conditions [10].

While the simulation of tunnel convergence in single tunnels has been widely investigated and reported in published literature, few works have addressed the computational evaluation of deformation in twin tunnels. Less attention has been dedicated to assessing the mutual mechanical interaction induced by the excavation of the transverse gallery connecting the twin tunnels.

In this context, the main contributions of this paper may be summarized at both the material and tunnel analysis levels. At the material level, the constitutive state equations of the rock mass are formulated within the framework of coupled plasticity-viscoplasticity, which is relevant for clayey rocks. Such a framework allows capturing the irreversible instantaneous tunnel response (plasticity) as well as the delayed irreversible response (viscoplasticity). As regards the mechanical behavior of concrete material defining the lining, which is classically modeled through linear elastic relationships, the present analysis considers an aging viscoelastic rheological model relying upon the Bažant and Prasannan Solidification theory [3; 4]. At the structure analysis level, the simulation of deformation in the highly interacting material system components (namely, rock mass and lining), resulting from the excavation process of twin tunnels and transverse gallery, is handled using finite element simulations performed in a three-dimensional setting. The 3D finite element model is essential for this analysis as it not only can represent a complex domain (such as the connection between longitudinal and transverse tunnels) but also enables simulation of the excavation process and lining placement through the activation-deactivation method.

From the computational viewpoint, the constitutive models formulated for the rock mass and lining constituent are implemented into the same software utilizing the UPF/USERMAT customization tool [2] of ANSYS standard software, together with the related numerical integration schemes. In this context, the finite element analysis specifically investigates the three-dimensional interaction induced by the construction process, twin tunnels proximity, and the presence of the transverse gallery.

2. Fundamental assumptions

The basic assumptions of the constitutive and computational modeling, as well as related limitations, are summarized as follows:

(a) Only the configuration of deep tunnels shall be considered in the subsequent analysis, thus neglecting deformations caused by surface loads and settlements arising from the excavation process;
(b) Although material heterogeneity and behavior anisotropy are inherent features of soils and rocks, the rock mass is modeled throughout the paper as a homogeneous and isotropic continuous medium. At the scale adopted for tunnel modeling (macroscopic scale), this assumption means in particular that the possible micro-heterogeneities, such isotropic distributions of joints or cracks present at the finer scale, are accounted for in the homogenized behavior by means of a preliminary homogenization process (e.g., [20, 14, 7, 19, 1]). Clearly enough, the framework of continuum modeling adopted in the paper would reveal questionable when the rock mass is cut by a few macro-scale fracture joints;
(c) The rock mass is phenomenologically modeled using an elastoplastic-viscoplastic rheological law to capture instantaneous and long-term responses. This approach disregards the aspect connected temperature gradients, water flow, and poromechanics coupling;
(d) Despite the complexity of the stress distribution prevailing in the rock mass before the process of tunnel excavation, which is mainly affected by the geological history, the present study assumes a geostatic initial stress reflected by an isotropic state of stress.
(e) Twin tunnels are often designed considering a time gap between excavation fronts. However, the finite element simulations assume synchronous excavation steps to ensure symmetry conditions.
(f) The simulation excavation processes are curried out assuming a constant tunnel advancement rate (i.e., constant excavation speed), together with a constant thickness of concrete lining.
(g) Effects of temperature and humidity that may affect the viscoelastic behaviour of concrete lining are disregarded.
(h) Perfect bonding is assumed at the interface between concrete lining and the rock mas.
(i) The framework of infinitesimal strain analysis, together with quasi-static evolutions, is adopted in the paper. In particular, dynamic excitations and related inertial forces, such as those induced, for instance, by earthquakes or explosions, shall not be considered in the numerical analysis.

3. Constitutive Model of the Rock Material

For many deep clay rock formations, the time-dependent phenomenon holds significant importance. And viscoplastic models are traditionally used for this modeling. However, viscoplastic models alone fail to consider the potential failure during the stages of excavation. Indeed, during this early stage, the rock mass is subjected to severe loads and high strain rates which can affect the long-term response. In such scenarios, the incorporation of coupled plasticity allows the consideration of the redistribution of stresses due to failure process. This study will adopt the elastoplastic-viscoplastic model initially developed by Rousset in his investigation of radioactive waste repositories in Boom clay [21,28]. Other subsequent studies considering this feature in single tunnels are in [6, 23, 16] and only a summary of this model will be presented here. More details, including validations and its application in a single tunnel also can be found in [27]. For details of the implementation of this model at USERMAT, see [25].

This elastoplastic-viscoplastic model is formulated based on a serial association of the elastoplastic and viscoplastic constitutive models. The local strain rate $\dot{\boldsymbol{\varepsilon}}$ is split into three contributions $\dot{\boldsymbol{\varepsilon}} = \dot{\boldsymbol{\varepsilon}}^e + \dot{\boldsymbol{\varepsilon}}^p + \dot{\boldsymbol{\varepsilon}}^{vp}$, so that the constitutive relationships relating the Cauchy stress rate $\dot{\boldsymbol{\sigma}}$ and strain rate components can be written as:

$$\dot{\boldsymbol{\sigma}} = \boldsymbol{D} : \dot{\boldsymbol{\varepsilon}}^e = \boldsymbol{D} : (\dot{\boldsymbol{\varepsilon}} - \dot{\boldsymbol{\varepsilon}}^p - \dot{\boldsymbol{\varepsilon}}^{vp}). \tag{1}$$

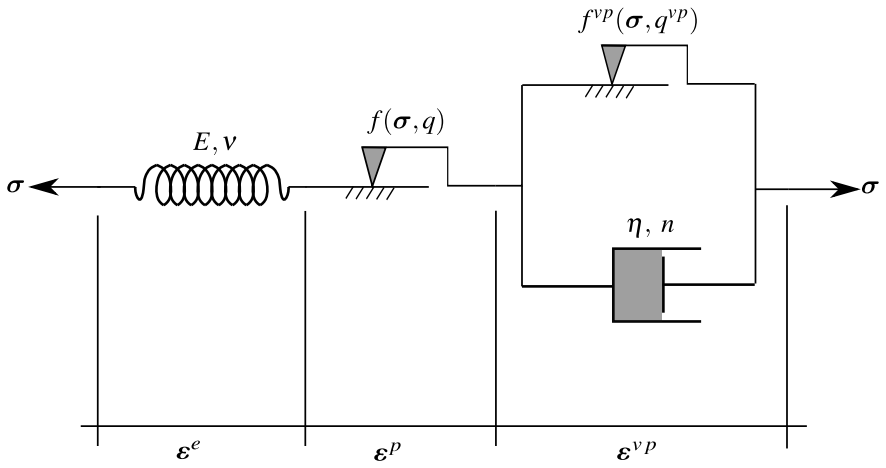

Figure 1: Rheological representation of the elastoplastic-viscoplastic model.

In the above relationship, $\dot{\boldsymbol{\varepsilon}}^e$, $\dot{\boldsymbol{\varepsilon}}^p$ and $\dot{\boldsymbol{\varepsilon}}^{vp}$, represent respectively the elastic, plastic and viscoplastic strain rate, and $\boldsymbol{D}$ denote the fourth-order isotropic elastic linear constitutive tensor. The one-dimensional representation in Fig. 1 shows this association. In this model is used a Drucker-Prager plastic flow surface given by

$$f(\boldsymbol{\sigma}, q) = f(I_1, J_2, q) = \beta_1 I_1 + \beta_2 \sqrt{J_2} - q(\alpha), \tag{2}$$

which I_1 is the first invariant of the stress tensor, J_2 the second invariant of the deviator tensor and β_1, β_2 and $q(\alpha)$ are strength parameters related to the friction angle ϕ and cohesion $c(\alpha)$, respectively. In the present model Drucker-Prager surface been inner of the Mohr-Coulomb surface [5], that is,

$$\beta_1 = \frac{(k-1)}{3}, \quad \beta_2 = \frac{(2k+1)}{\sqrt{3}}, \quad q(\alpha) = 2\sqrt{k}\, c(\alpha), \tag{3}$$

where $k = (1 + \sin\phi)/(1 - \sin\phi)$. The internal variable α is the equivalent plastic strain $\bar{\varepsilon}^p$ used to simulate strain hardening/softening phenomena. However, for this study, we adopt perfect plasticity, meaning that c is a constant. For the viscoplasticity surface f^{vp} the same surface is empolyed, but with ϕ^{vp} in β_1 and β_2, and $q^{vp} = 2\sqrt{k^{vp}} - c^{vp}$ where $k^{vp} = (1 + \sin\phi^{vp})/(1 - \sin\phi^{vp})$ and c^{vp} is a constant, i.e., perfect viscoplasticity. The plastic flow rule is given by:

$$\dot{\boldsymbol{\varepsilon}}^p = \begin{cases} \dot{\lambda}\dfrac{\partial g}{\partial \boldsymbol{\sigma}} & \text{for } f > 0 \\ \mathbf{0}, & \text{for } f \leq 0 \end{cases}, \tag{4}$$

where $\dot{\lambda}$ is the plasticity multiplier and g is a potential flow function analogous to f used to simulate the volume dilatation during the evolution of plastic deformations. However, for this analysis, was used associated plasticity, i.e., $g = f$. The plastic multiplier is obtained through the consistency condition $\dot{f} = 0$. Numerical details of this implementation can be found in [27]. For viscoplastic flow rule we have,

$$\dot{\boldsymbol{\varepsilon}}^{vp} = \dot{\lambda}^{vp}\frac{\partial f^{vp}}{\partial \boldsymbol{\sigma}} \tag{5}$$

In contrast to the plastic multiplier, the viscoplastic multiplier λ^{vp} is independent of a consistency like condition. As a result, its expression is explicit. Based on the framework of generalized Perzyna's overstress theory [22], its expression may derived as follows:

$$\dot{\lambda}^{vp} = \frac{\Phi(\boldsymbol{\sigma}, q^{vp})}{\eta} \quad \text{and} \quad \Phi = \left\langle \frac{f^{vp}(\boldsymbol{\sigma}, q^{vp})}{f_0} \right\rangle^n, \tag{6}$$

where Φ is the overstress function, η is the dynamic viscosity constant, n is the dimensionless parameter that gives the form of the power law, f_0 a parameter conveniently adopted and $\langle * \rangle$ is the McCauley function which is 0 when $* < 0$, i.e. viscoplastic flow will only occur when the overstress function is positive.

In this coupled model, when $\phi = \phi^{vp}$, cohesion entirely controls the evolution of local mechanical fields. Specifically, when $c \to \infty$ and $c^{vp} \to \infty$, the system achieves a purely elastic solution. The solution becomes purely elastoviscoplastic with $c \to \infty$, while a pure elastoplastic solution emerges with $c^{vp} \to \infty$. In the coupled analysis, condition $c^{vp} < c$ is adopted, allowing the viscoplastic domain to occur without plasticity. However, in the presence of plasticity, viscous effects become inevitable. Fig. 2 illustrates these domains in principal stress space.

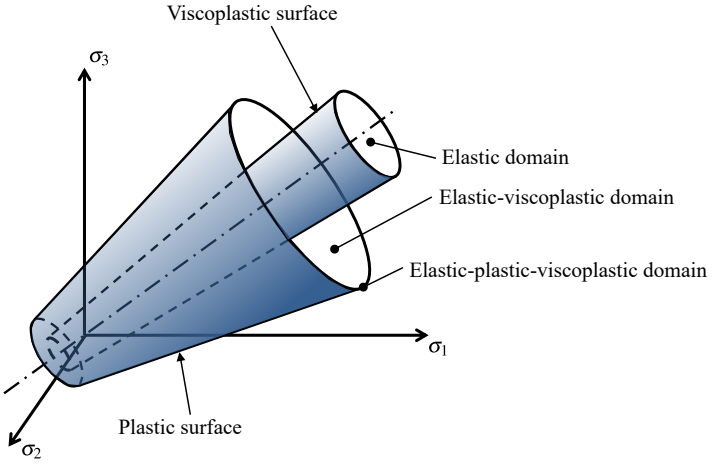

Figure 2: Elastoplastic-viscoplastic domains.

4. Constitutive Model of the Lining

In a phenomenological way, the creep in the concrete represents a dimensional change in the material under the influence of the sustained loading while shrinkage is the decrease in volume caused by drying. Creep and shrinkage are complex phenomena and have a considerable effect on the performance of the concrete lining and in the long-term convergence of a tunnel, causing strain and stress distribution around the cavity of the tunnel. We implemented a concrete creep through a Generalized Kelvin chain, based on Bažant and Prasannan's Solidification Theory [3, 4], with model parameter adjustments performed using the CEB-FIP MC90 formulation present in [8]. Only a summary of this model will be presented. More details, including validations and their application in a single tunnel can be found in [26] and details of the implementation at USERMAT are in [24].

Therefore, in this model, the constitutive relationship between stress and strain is

$$\dot{\boldsymbol{\sigma}} = \boldsymbol{D} : \dot{\boldsymbol{\varepsilon}}^{e} = \boldsymbol{D} : \dot{\boldsymbol{\varepsilon}} - \boldsymbol{D} : \dot{\boldsymbol{\varepsilon}}^{sh} - \boldsymbol{D}^{*} : \dot{\boldsymbol{\varepsilon}}^{cr} \tag{7}$$

where $\dot{\boldsymbol{\varepsilon}}^{sh}$ and $\dot{\boldsymbol{\varepsilon}}^{cr}$ are the shrinkage and creep strain rate, respectively, while $\boldsymbol{D}$ and $\boldsymbol{D}^{*}$ denote the fourth-order isotropic elastic linear constitutive tensor and modified constitutive tensor that incorporates the aging of the concrete, respectively. Due to the time solution procedure the incremental relationship of the Eq. (7) is given by:

$$\Delta\boldsymbol{\sigma} = \boldsymbol{D} : \Delta\boldsymbol{\varepsilon} - \boldsymbol{D} : \Delta\boldsymbol{\varepsilon}^{sh} - \boldsymbol{D}^{*} : \Delta\boldsymbol{\varepsilon}^{cr} \tag{8}$$

in which the increment of shrinkage strain is:

$$\Delta\boldsymbol{\varepsilon}^{sh} = \Delta\varepsilon_{sh}(t_s)\mathbf{1} \tag{9}$$

where t_s represents the concrete curing time, and $\Delta\varepsilon_{sh}$ is the variation of magnitude of the concrete deformation by shrinkage, determined using the expressions of CEB-FIP MC90 [8]. To calculate the increment of creep strain, denoted as $\Delta\boldsymbol{\varepsilon}^{cr}$, we use the incremental algorithm developed by Bažant and Prasannan [3; 4], with an adjustment to incorporate CEB-FIP MC90 formulation. This adaptation is possible comparing the creep functions $\boldsymbol{J}(t, t_0)$ of both references. This gives to the following equivalence:

$$E_0 = E_c(t_0),\ \gamma_c(t - t_0) = \beta_c(t - t_0),\ \frac{1}{\upsilon(t)} = \frac{\phi_0}{E_{ci}} \text{ and } \frac{1}{\eta(t)} = 0 \tag{10}$$

in which, according to Bažant and Prasannan [3; 4], E_0 is the modulus of elasticity of the concrete aggregates togheter with the microscopic particles of the cement paste, $\gamma_c(t-t_0)$ is the microviscoelastic deformation of the volume fraction of solidified concrete $v(t)$, $\eta(t)$ is the apparent macroscopic viscosity and, according to CEB-FIP MC90 [8], $E_c(t_0)$ is the tangent elastic modulus of the concrete at the instant of loading application t_0, $\beta_c(t-t_0)$ is a coefficient that depends on the loading age $t-t_0$, ϕ_0 is a coefficient that depends on the age of the concrete at the instant of loading application and E_{ci} the tangent elasticity modulus of the concrete at the age of 28 day.

5. Spatial and time discretization of the domain

The problem domain Ω consists of a twin deep tunnel with a cross gallery, as shown in Fig. 3.

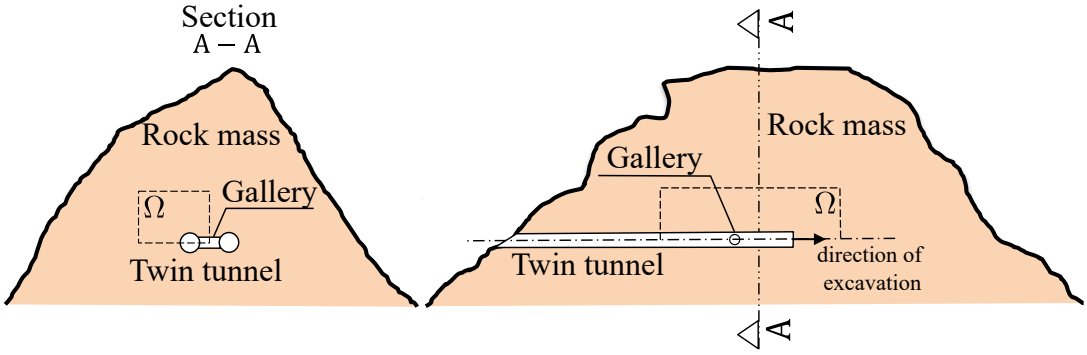

Figure 3: Problem domain

This domain is parameterized based on the radius of the longitudinal tunnel R_i. The geometric parameters and boundary conditions for the domain problem are shown in Fig. 4. We considered front, side, and bottom symmetry to reduce computational cost. In this domain, d_1 is the distance between longitudinal tunnel axes, L_2 total excavated length, d_3 domain height, L_1 length of the unexcavated region, L_3 transversal length of the domain, L_p step length of the excavation process, d_2 position of the gallery along the longitudinal tunnel. In conjunction with boundary pressure σ_x, σ_y and σ_z, we apply the initial stress condition $\boldsymbol{\sigma}_0 = -\sigma_x \boldsymbol{e}_x \otimes \boldsymbol{e}_x - \sigma_y \boldsymbol{e}_y \otimes \boldsymbol{e}_y - \sigma_z \boldsymbol{e}_z \otimes \boldsymbol{e}_z$ at all integration points to simulate the initial state of the rock mass. The spatial discretization in Fig. 4 corresponds to a mesh with trilinear hexahedral elements (SOLID 185, 8 nodes), except in the gallery region, which uses higher-order tetrahedral elements (SOLID186, 10 nodes). We divided the mesh into two regions: one near the tunnel (light gray), which we refined more, and a region farther away (dark gray), which we increased the aspect ratio to minimize the number of elements in that region. Due to the low deformation gradient away from the tunnel wall, elements in this area can be considerably larger than in other regions. Fig. 5 presents the mesh at the cross-section of the longitudinal tunnel, with e representing the thickness of the lining.